Naor, P., and R. Shinnar, *Ind. Eng. Chem. Fundamentals*, 2, 4, 278 (1963).
Rescigno, A., and G. Segre, *Drugs and Tracer Kinetics*, Blaisdell Publishing Co., Mass. (1966).
Rissanen, J., *SIAM J. Contr.*, 9, 3, 420 (1971).
Rossen, R. H., Ph.D. thesis, Princeton Univ., N.J. (1972).
Schiesser, W. E., Ph.D. thesis, Princeton Univ., N.J. (1959).
Sheppard, C. W., *Basic Principles of the Tracer Method*, Wiley, New York (1962).
Silverman, L. M., *IEEE Trans. Auto. Contr. AC-16*, 6, 554 (1971).
Tether, A. J., *IEEE Trans. Auto. Contr. AC-15*, 4, 427 (1970).
van Swaaij, W. P., J. C. Charpentier, and J. Villermaux, *Chem. Eng. Sci.*, 24, 1083 (1969).
Widder, D. V., *The Laplace Transform*, Princeton Univ. Press, N.J. (1946).
Wilkinson, J. H., *The Algebraic Eigenvalue Problem*, Clarendon Press, Oxford (1965).
Willems, J. C., *Archives for Rational Mech.*, 45, 5, 352 (1972).

Manuscript received September 15, 1975; revision received and accepted November 25, 1975.

Fluid and Particle Entrainment Into Vertical Jets in Fluidized Beds

J. M. D. MERRY
Westinghouse Research Laboratories
Pittsburgh, Pennsylvania 15235

The flow of particles and fluid in the vicinity of vertical jets in fluidized beds was studied by using a two-dimensional bed of lead shot fluidized by water. It was found that both interstitial fluid and solid particles are entrained into the jet as it expands and penetrates into the bed. An approximate mathematical model is developed to describe the particle and fluid flow fields observed experimentally; from this, an expression is derived for rates of entrainment into vertical jets in fluidized beds, and a model is postulated for the flow fields around grid jets.

SCOPE

Fluid issuing from the distributor plate at the base of a fluidized bed takes the form of a dilute phase torch or jet which penetrates into the bed of particles. For processes involving chemical reaction, heat transfer, or mass transfer, the mechanism of the jetting region can be extremely important (Behie and Kehoe, 1973; Toei, 1973; Halow, 1974), yet, despite extensive literature on fluidization, little attention has been focused on this region of the bed.

In the multistage fluidized bed coal gasification processes (Lemezis and Archer, 1973), the combustion zone for process heat generation is often a vertical air jet in the lower leg of the combustor/gasifier vessel, into which char fines are fed. This lower leg also acts as the residual ash agglomerator, and the mean particle size there will be considerably larger than the mean size of the injected char fines. It was reasoned that the fines would tend to follow the path of the interstitial fluid rather than that of the larger agglomerates. To discover the likely route of the injected fines and so determine how best to feed fines to the bed so that they would be carried into the combustion jet, an experiment was set up to investigate the flow of interstitial fluid in the vicinity of a vertical jet in an incipiently fluidized bed.

This work has resulted in a better understanding of jet behavior in fluidized beds, and the insight gained has been used in developing a conceptual design for a commercial combustor/gasifier (Merry et al., 1975). A mathematical model of the flow fields around the jet leads to an approximate expression for estimating rates of entrainment of fluid and particles into the jet, and this in turn could lead to improved modeling of the jetting regions of fluidized beds. Application of the model is illustrated by using two examples from the literature.

CONCLUSIONS AND SIGNIFICANCE

An experimental investigation of vertical water jets into a two-dimensional water fluidized bed of lead shot has revealed that interstitial fluid as well as solid particles are entrained into the jet stream as the jet expands and penetrates into the bed. There appears to be a dividing streamline in the fluid such that all the fluid inside this streamline is entrained into the jet, while the fluid outside bypasses the jet and continues to flow upward through the bed. Fine particles or fluid which are to be fed into the jet should be injected inside the dividing streamline in the fluid. The appearance of the jet and the motion of the particles in the liquid-solid system are very similar to the reported observations of Markhevka et al. (1971) and Zenz (1968, 1971) for gas-solid systems, and it is considered that the results presented here will apply equally to either fluid-solid combination.

By representing the effect of the jet on fluid and particle motion in the particulate phase of the bed by a sink, an approximate two-dimensional mathematical model has been developed which describes the solid particle and interstitial fluid flow fields around the jet. This successfully predicts the experimentally observed positions of the dividing streamline in the fluid.

The rate of entrainment of particles and fluid into the jet is directly related to the strength of the sink representing the effect of the jet. By making some simplifying assumptions to the mathematical model, an algebraic expression [Equation (8)] is obtained from which reasonable estimates can be made for the rates of particle and fluid entrainment into two-dimensional and axisymmetric vertical jets in fluidized beds. This expression is

J. M. D. Merry is with the Computer Aided Design Centre, Madingley Road, Cambridge CB3 OHB England.

thought to be the first of its kind, and it could provide important information for modeling jetting regions in fluidized beds; it indicates that specific entrainment rate, that is, entrainment rate per unit area of nozzle cross section, increases with u_{mf} and with L/d_o.

A model is postulated for the flow around grid jets in fluidized beds which suggests that interstitial fluid is recirculated around grid jets just as it is near the gas inlet in a spouted bed (van Velzen, 1974). Fluid recirculation around the jet continues around the subsequently formed bubble giving rise to the cloud around a rising bubble in a fluidized bed (Rowe, 1971); it could be an important factor where chemical reaction or mass transfer occur in the jet.

Several workers have reported that solid particles from the bed are entrained into jets in fluidized beds, but there is little reference to the corresponding motion of the interstitial fluid in the particulate phase. Zenz (1968) has studied vertical jets in fluidized beds, and he illustrates how the jets and subsequent bubbles are formed at orifice holes (Zenz, 1971). Markhevka et al. (1971) studied motion pictures of vertical jets at the wall of a cylindrical bed and observed that the bottom region of the jet is conical and that bubbles form in a regular pattern at the end of the jet. The upper ellipsoidal part of the jet, above the conical region, elongates, takes the form of a bubble, and separates from the jet. The jet then collapses and the cycle is repeated, so that the jet region expands before and during bubble growth and contracts after bubble separation in a rhythmic, pulsating cycle. They found that the length y_c of the lower conical section is related to the jet length L by

$$y_c/L = 0.55 \tag{1}$$

Solid particles collapse into the lower region of the jet, are accelerated in the jet stream, and are carried to the top of the jet where they return to the bed. Kozin and Baskakov (1967) studied horizontal jets from a bubble cap distributor and observed similiar particle entrainment into the jet near the nozzle, leading to a pattern of solids circulation in the adjacent particulate phase, and Shakhova (1968) and Merry (1971) have reported solid particle entrainment into horizontal jets in incipiently fluidized beds.

It is well known that the expansion of a homogeneous jet is supported by entrainment of fluid into the jet stream (Abramovich, 1963). Since the profile of the jet region in a fluidized bed is similar to that of a homogeneous jet into a counterflowing stream (Merry, 1971; Vulis and Leont'yeva, 1955), it seemed likely that interstitial fluid as well as solid particles would be entrained into the jet. The results presented here show that this is so, and an approximate mathematical model is set up to predict the solid particle and interstitial fluid streamlines in the particulate phase around the jet.

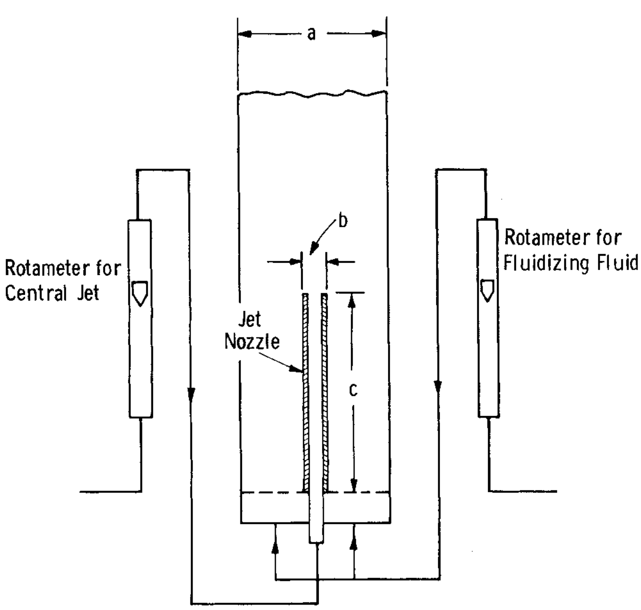

Fig. 1. Schematic layout of two-dimensional bed used to study flow patterns around a vertical jet in a fluidized bed. a = 305 mm, b = 44.5 mm, c = 380 mm.

VERTICAL JET IN A TWO-DIMENSIONAL FLUIDIZED BED

Experiment

The flow of solid particles and interstitial fluid in the vicinity of a vertical jet was studied in a two-dimensional fluidized bed 305 mm wide and 12.7 mm thick, which was made by separating two Plexiglas sheets with 12.7 mm spacers. The apparatus is shown schematically in Figure 1. The centrally positioned jet nozzle was 19.1 mm wide on the inside and 44.5 mm wide on the outside and extended 380 mm above the fluid distribution plate. There were separate fluid supplies to the jet and to the bed region adjacent to the nozzle, and each was metered by a rotameter. The bed was operated with a depth of around 450 mm above the end of the nozzle, with the particles in the region adjacent to the nozzle incipiently fluidized.

The aim of the experiment was to inject a colored dye into the interstitial fluid adjacent to the nozzle at a point below the end of the nozzle and to record its subsequent motion photographically. To facilitate the experimental procedure, it was decided to use lead shot as the bed material and water as the fluidizing fluid. Lead shot was chosen since it exhibits aggregative (or bubbling) fluidization when fluidized by water, as in a typical gas-solid fluidized bed. A white dye (water soluble paint) was injected through self-sealing ports in the back wall of the bed into the interstitial water, and either still photographs or motion pictures were taken through the front wall. Typical photographs are shown in Figure 2 for a bed of 1 mm lead shot and in Figure 3 for a bed of 2 mm lead shot. The experimental conditions relating to these photographs are given in Table 1.

Dye injected at ports adjacent to the nozzle, Figures 2*a* and 3*a*, tended to be swept into the jet stream, whereas dye injected at ports distant from the nozzle, Figures 2*b* and 3*b*, tended to bypass the jet stream. This was the pattern observed in all experiments, indicating the presence of a dividing streamline in the fluid flow field around the jet; the fluid inside the dividing streamline is entrained into the jet, and the fluid outside bypasses the jet and continues to flow upward through the bed.

The movement of the solids in the vicinity of the jet can also be seen in Figures 2 and 3. There is some particle movement in the region adjacent to the nozzle because of some inevitable nonuniformity of fluidization there, but the more intense particle motion takes place above the end of the nozzle. Particles are picked up by

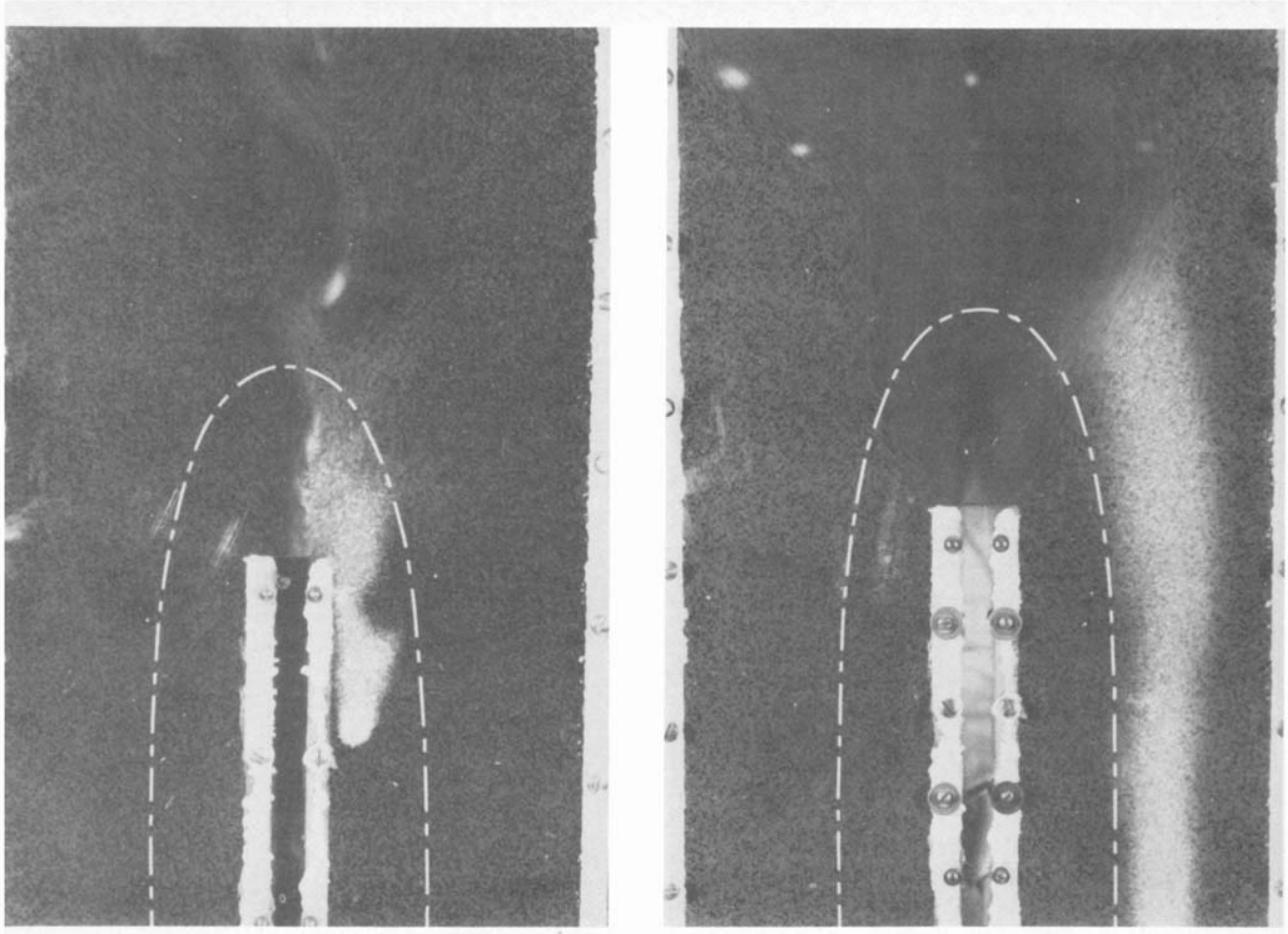

a b

Fig. 2. Vertical water jet issuing into bed of 1 mm lead shot fluidized by water, experiment 1, $u_0 = 1.37$ m/s. Chain line is predicted position of dividing streamline in fluid. *a*. Dye injected adjacent to nozzle flows into jet. *b*. Dye injected distant from nozzle bypasses jet.

TABLE 1. CONDITIONS OF EXPERIMENTS IN BED OF LEAD SHOT FLUIDIZED BY WATER

Experiment number	1	2	3	4
Particle diameter, d_p, mm		1		2
Absolute incipient fluidizing velocity, u_{mf}, mm/s		146		204
Jet nozzle velocity, μ_o, m/s	1.37	2.74	3.96	2.44
Predicted jet penetration depth, equation (32),* L, mm	143	235	293	214

the jet stream and carried to the top of the jet; these are replaced by other particles moving from the particulate phase towards the jet. Steady particle circulation sets in, characterized by a downward particle movement in the particulate phase adjacent to the jet. This movement extends through practically all of the bed above the end of the nozzle, but the highest velocities occur in a conical region surrounding the jet. Bubbles form above the jet, imparting a vortex motion to the particles in the upper part of the bed. The boundary of the conical region passes through the top outer edge of the nozzle and subtends an angle α with the horizontal. In the experiments conducted, the angle α was independent of nozzle velocity and particle size, with a magnitude of approximately 65 deg., corresponding to the angle of internal friction of the solids (Zenz and Othmer, 1960).

The particle motion is very similar to that observed by Markhevka et al (1971) with vertical jets in gas-solid fluidized beds. In addition, the experiments above have shown that interstitial fluid as well as solid particles are entrained into a vertical jet in a fluidized bed. Fine particles or fluid which are to be fed into the jet should be injected inside the dividing streamline in the fluid.

Theory

The phenomenon of the dividing streamline in the fluid observed experimentally is reminiscent of the flow field due to a source or sink in a uniform stream (Milne Thomson, 1968, p. 211). An approximate two-dimensional model has been developed to describe the motion of particles and fluid in the particulate phase in the vicinity of the jet by using a sink to represent mathematically the effect of the jet on this motion. Details of the derivation are given in the Appendix.* The model uses the technique of Davidson and Harrison (1963), whereby the solid phase and the interstitial fluid phase are treated separately, as if each was an incompressible, inviscid continuum. This yields a relationship [Equation (18)*] between the particle stream function ψ_p and the interstitial fluid stream function ψ_f; namely

$$\psi_f - \psi_p = u_{mf} \cdot x \qquad (2)$$

The effect of the jet on the motion of the particulate phase is represented by a sink, and the physical presence of the bed walls and base and of the jet nozzle is represented by superimposing rows of sources and sinks.

The resulting particle stream function is given by Equation (23) as [Appendix*]

$$\psi_p = m_1 \cdot \theta_1 + m_2(\theta_2 - \theta_o) \qquad (3)$$

where m_1 and m_2 are the strengths of sinks representing

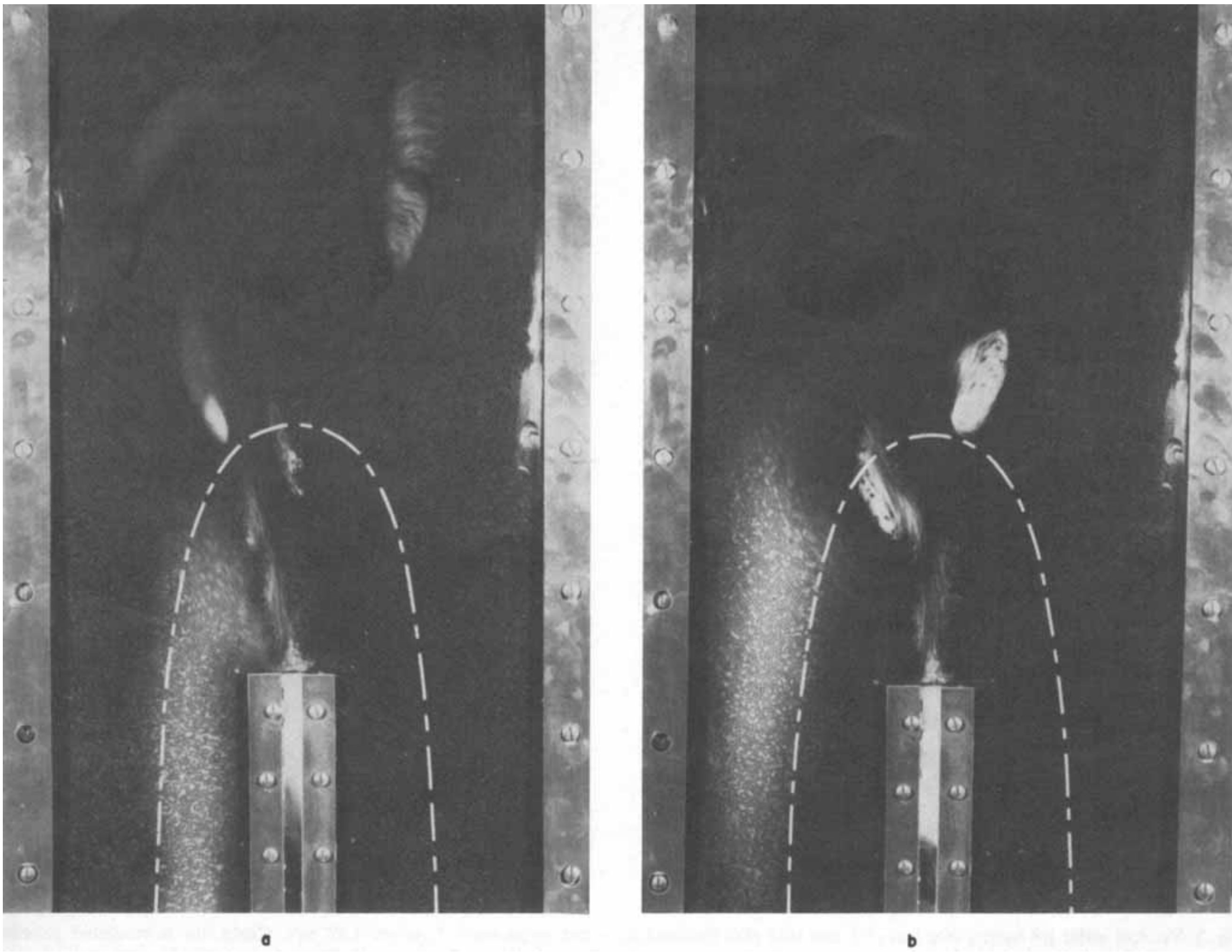

Fig. 3. Vertical water jet issuing into bed of 2 mm lead shot fluidized by water, experiment 4, $u_0 = 2.44$ m/s. Chain line is predicted position of dividing streamline in fluid. *a.* Dye injected adjacent to nozzle flows into jet. *b.* Dye injected distant from nozzle bypasses jet.

TABLE 2. DEDUCED PARAMETERS FOR THEORETICAL MODEL. EXPERIMENT NUMBERS CORRESPOND TO THOSE IN TABLE 1

Experiment number	1	2	3	4
Positions $(y_1 - c)$ mm	69	123	156	108
of sinks $(c - y_2)$ mm	5.6	5.8	6.1	5.8
(u_{mf}/m_1) mm^{-1}	0.051	0.042	0.038	0.044
m_1 mm^2/s	2 860	3 480	3 870	4 630
m_2 mm^2/s		1 030		1 440
Wall stream function (ψ_{fw}/m_1)	7.79	6.40	5.76	6.74
Ratio $\left(\dfrac{\text{fluid entrained}}{\text{fluid supplied to nozzle}}\right)$ %	31	19	14	28

the jet and the nozzle, respectively, and θ_o, θ_1, and θ_2 are angles defined by [Equation (24), Appendix]*

$$\theta_n = \tan^{-1}\left[\tanh\frac{\pi}{a}(y - y_n)\cot\frac{\pi x}{a}\right] + \tan^{-1}\left[\tanh\frac{\pi}{a}(y + y_n)\cot\frac{\pi x}{a}\right]$$

for $n = 0, 1$, or 2, and $y_o = 0$.

From Equations (2) and (3), the interstitial fluid stream function is given as

$$\psi_f = u_{mf}\cdot x + m_1\cdot\theta_1 + m_2(\theta_2 - \theta_o) \qquad (4)$$

Equation (4) indicates that the interstitial fluid flow field is characterized by the flow due to a sink in a uniform velocity stream.

* Supplementary material has been deposited as Document No. 02753 with the National Auxiliary Publications Service (NAPS), c/o Microfiche Publications, 440 Park Ave. South, New York, N. Y. 10016 and may be obtained for \$3.00 for microfiche or \$5.00 for photocopies.

Results and Discussion

Methods adopted for estimating values for the parameters which define the model are presented in the Appendix,* and values of the parameters corresponding to experiments 1 to 4 are given in Table 2. The predicted positions of the dividing streamline in the fluid for experiments 1 and 4 are shown as chain lines in Figures 2 and 3, respectively, and the predicted streamlines for the whole flow field are shown in Figure 4 for the conditions of experiment 4 with 2 mm lead shot; the full lines are the particle streamlines, the broken lines are the interstitial fluid streamlines, and the chain lines represent the nozzle wall $(\psi_{fo} = 0)$ and the dividing streamline $(\psi_{fd} = \pi m_1)$ in the fluid flow field. The ratio of the flow rate of fluid entrained into the jet to the flow rate of

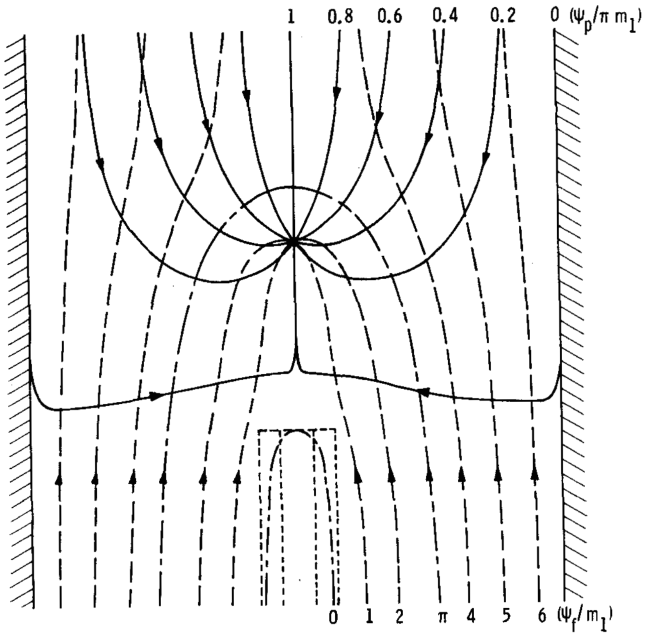

Fig. 4. Predicted streamlines for flow around vertical jet, corresponding to experiment 4 with 2 mm lead shot. Full lines are particle streamlines [Equation (3)], broken lines are interstitial fluid streamlines [Equation (4)], and chain lines represent the nozzle wall ($\psi_{fo} = 0$) and the dividing streamline in the fluid ($\psi_{fd} = \pi m_1$).

fluid supplied to the jet nozzle is also given in Table 2. This ratio lies between 14 and 31% for the four experiments reported.

The mathematical model is at best a simple approximation of the very complex phenomena which occur as a fluid jet issues into a fluidized bed. Several objections to the approach adopted may be raised, and the more obvious ones are outlined below.

The motion of particles and fluid around the jet is actually controlled by three complementary components: the fluid flow out of the jet nozzle, the entrainment flow into the base of the jet, and the flow due to bubbles leaving the end of the jet. This model represents only one of these components, the entrainment into the bottom of the jet. Motion in the jet and in and around the subsequent bubbles is not accounted for at all. This is to be expected, for the technique of treating fluid and solids separately is only applicable to the dense particulate phase; the model breaks down when the material crosses into the dilute phase jet stream. To include the other two components as well is very much more complicated than what has been attempted here, and it was considered that the additional complexity was not justified at this stage.

Representing the effect of the jet on the motion of the particulate material by a hypothetical sink suggests that the particles and fluid entrained into the jet disappear into the sink and are removed from the bed. This is clearly not the case; entrained particles and fluid are accelerated in the jet stream and carried to the end of the jet whence they return to the bed either directly to the particulate phase or else to the bubble and its wake which form above the jet. There is a regular flow of particles and fluid into the bottom of the jet and out of the top.

Similarly, the concept of the dividing streamline in the fluid is only applicable to the particulate phase adjacent to the jet. The dividing streamline ceases to exist when it meets the boundary of the jet, and the supposed stagnation point in the fluid on the jet axis (see Appendix* and Figure 9) does not occur in reality.

However, the predicted flow pattern of solid particles and interstitial fluid (Figure 4) is a fair representation of what actually takes place in the particulate phase adjacent to the base of the jet, and, in particular, the predicted position of the dividing streamline in the fluid corresponds closely with the experimental observations up to the point where the fluid meets the jet boundary.

Justification of the model really lies in its ability to predict the positions of the dividing streamline in the interstitial fluid; for the experiments 1 to 3 with 1 mm lead shot and u_o = 1.37, 2.74 and 3.96 m/s, respectively, the dye flow patterns are shown in Figure 5*a*, *b*, and *c*. At first sight, the fluid flow patterns and the dividing streamlines (chain lines) seem to be almost identical, but when the dividing streamlines are plotted on the same graph, Figure 5*d*, it is clear that they are different and that they do predict the experimentally observed trend. The dye was injected at the same point in each experiment. In Figure 5*a*, the dye travels outside the dividing streamline and will bypass the jet. As the nozzle velocity and the jet length are increased (Figure 5*b*), the dividing streamline moves outward so that the dye almost crosses it. With a further increase in the nozzle velocity (Figure 5*c*), the dividing streamline has moved out so far that it is within the dye tracer; some of the dye is swept into the jet and some bypasses it.

It may be argued that since the findings reported here are based on information obtained in liquid-solid fluidized beds, they are not necessarily applicable to gas-solid fluidized beds. However, fluid mechanic similarities between aggregatively fluidized liquid-solid and gas-solid beds have been demonstrated elsewhere (Davidson and Harrison, 1963; Merry and Davidson, 1973), and the appearance of the jet and the motion of the particles in the liquid-solid system are very similar to the reported observations of Markhevka et al. (1971) and Zenz (1968, 1971) for gas-solid systems. It is considered that the findings will apply equally well to either fluid-solid combination, although it should be emphasized that the model has been tested against a limited quantity of data only.

GRID JET IN A FLUIDIZED BED

Axisymmetric Jets

The work described above relates to two-dimensional jets in fluidized beds. Jets encountered in practice are generally three dimensional or axisymmetric, issuing from cylindrical nozzles rather than from two-dimensional slits. The experimental and theoretical techniques used above for two-dimensional jets become considerably more difficult when applied to the three-dimensional case, and instead a simple analysis is proposed for predicting entrainment into axisymmetric jets.

Assuming that the effect of the axisymmetric jet on the particulate phase can be represented by a three-dimensional sink of strength M_1, we may consider this sink to be made up of two-dimensional sinks of strength m_1, each effective in a narrow sector of the cylindrical bed of angle $\delta\theta$. The flow into each elemental sink will be given by $\delta q = \pi m_1\, d_o\, \delta\theta$, and by integrating from $\theta = 0$ to 2π, the total flow of fluid and particles into the sink M_1 is given as $q = 2\pi M_1 = 2\pi^2\, d_o\, m_1$. Therefore, the sink strength defining entrainment rate into the axisymmetric jet is related to that for the two-dimensional jet by

$$M_1 = \pi d_o\, m_1 \quad (5)$$

* See footnote on p. 318.

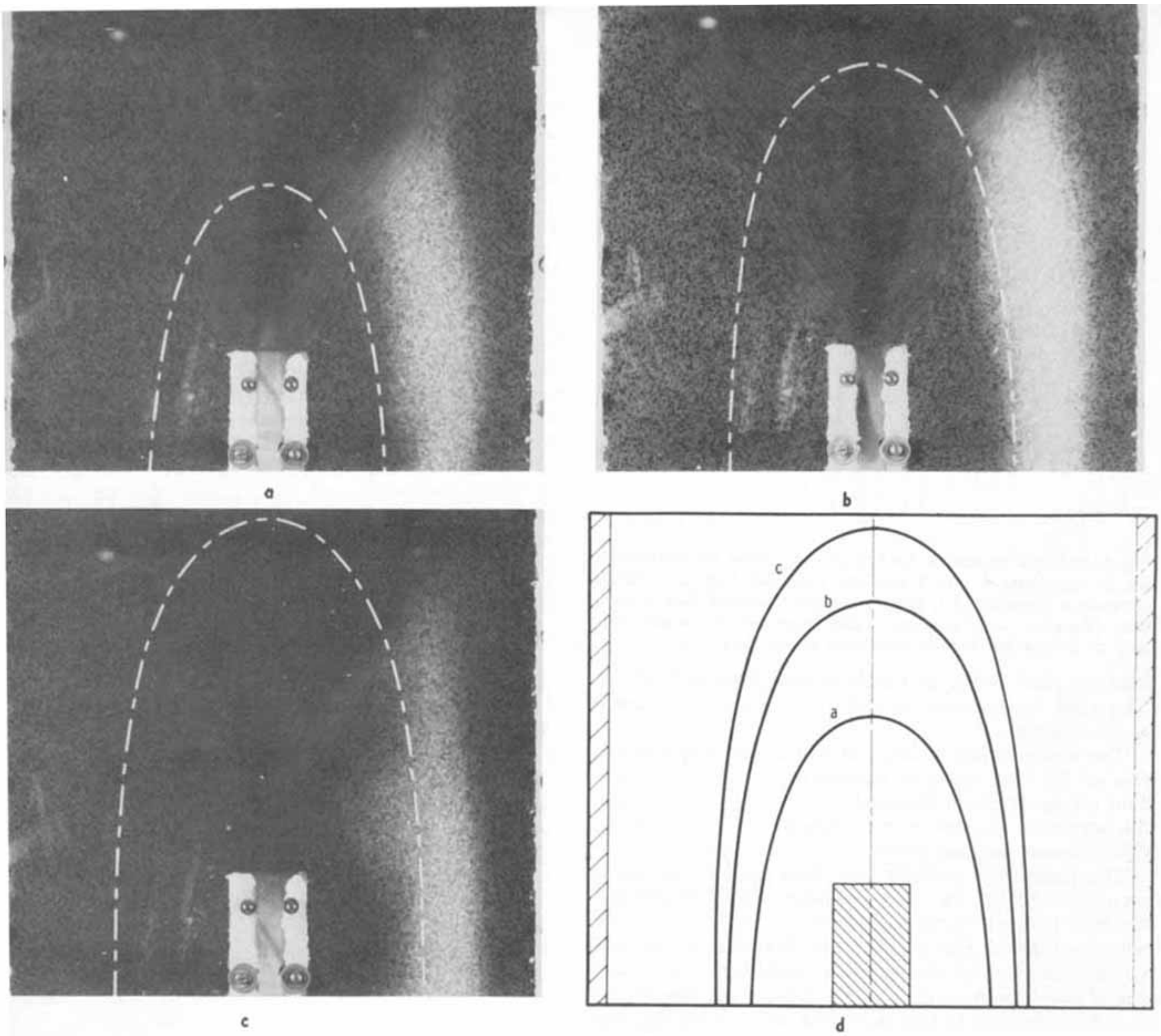

Fig. 5. Vertical water jets issuing into beds of 1 mm lead shot fluidized by water, showing how position of dividing streamline in fluid changes with jet nozzle velocity. *a*. Experiment 1, $u_0 = 1.37$ m/s. *b*. Experiment 2, $u_0 = 2.74$ m/s. *c*. Experiment 3, $u_0 = 3.96$ m/s. *d*. Positions of dividing streamline predicted by theoretical model.

Rate of Entrainment

The rate of entrainment into a jet is calculated as $q = 2\pi m_1$ for a two-dimensional jet and $q = 2\pi M_1$ for an axisymmetric jet. The entrainment flow rate q is made up of $\epsilon_{mf} \cdot q$ of interstitial fluid and $(1 - \epsilon_{mf})q$ of solid particles, where ϵ_{mf} is the bed voidage at incipient fluidization. Rates of entrainment into vertical jets can be predicted if values of m_1 or M_1 are known for given conditions.

By considering the theoretical model developed in the Appendix,* if the end of the jet nozzle is flush with the grid plate ($c = 0$, Figure 1), the mathematics can be simplified by putting $m_2 = 0$. Equation (4) for the interstitial fluid stream function can then be written as

$$\psi_f = u_{mf} \cdot x + m_1\theta_1 \qquad (6)$$

where

$$\theta_n = \tan^{-1}\left[\tanh\frac{\pi}{a}(y - y_n)\cot\frac{\pi x}{a}\right] + \tan^{-1}\left[\tanh\frac{\pi}{a}(y + y_n)\cot\frac{\pi x}{a}\right] \qquad (7)$$

y_1 is the height of the sink above the end of the nozzle, and by following a similar technique to that used in the Appendix,* an approximate analytical solution to Equation (6) can be obtained by assuming that $y_1 = L/2$ and that the dividing streamline ($\psi_f = \pi m_1$) in the fluid passes through the points $[\pm(d_o + L \cot \alpha)/2, L/2]$. Making these simplifying assumptions, we find that

$$\frac{2\,m_1}{d_o\,u_{mf}} = \left\{\frac{1 + \cot\alpha \cdot L/d_o}{\pi - \tan^{-1}\left[\tanh\frac{\pi L}{a}\cdot\cot\left[\frac{\pi d_o}{2a}(1 + \cot\alpha \cdot L/d_o)\right]\right]}\right\} \qquad (8)$$

Furthermore, for $L/a > 0.6$, $\tanh(\pi L/a) \sim 1$, and Equation (8) can be written

$$\frac{m_1}{d_o\,u_{mf}} = \frac{1 + \cot\alpha \cdot L/d_o}{\pi\,[1 + (1 + \cot\alpha \cdot L/d_o)\cdot d_o/a]} \qquad (9)$$

* See footnote on p. 318.

Values of $(m_1/d_o\ u_{mf})$ have been calculated from Equation (8) for a range of conditions which would apply to practical fluidized beds as follows:

$$a/d_o = 5 \text{ to } 40$$

$$L/d_o = 5 \text{ to } 60$$

$$\alpha = 55 \text{ to } 85 \text{ deg.}$$

The calculated values are plotted against $(1 + \cot \alpha \cdot L/d_o)$ for different values of (a/d_o) and are shown as full lines in Figure 6. The broken lines in Figure 6 have been obtained by solving the complete model (Appendix)* over the same range of variables, and these show how predictions made by the complete model differ from those of Equation (8). In general, the complete model predicts lower entrainment rates than Equation (8); agreement is within 15% and is very much closer over much of the range of variables considered. Equations (8) and (9) give virtually the same results for $L/a > 0.6$. For $L/a < 0.6$, Equation (9) predicts increasingly larger values of $(m_1/d_o\ u_{mf})$; for example, for $L/a = 0.2$, the difference is 10%.

Equation (8) is a straightforward algebraic expression which can be used to estimate rates of entrainment into vertical jets in fluidized beds. It is in close agreement with the more complicated complete model which requires numerical solution with a computer and is very much simpler to apply. It is thought to be the first expression of its kind and could provide important information for modeling jetting regions in fluidized beds. The rate of entrainment $(2\pi m_1)$ into the jet is determined by the physical size of the equipment (a, d_o), the length of the jet (L), the nozzle velocity [u_o, through Equation (32)*], and the properties of the bed material and fluid [d_p, ρ_p, ρ_f, d, μ through u_{mf} calculated following Kunii and Levenspiel (1969) and through L calculated by Equation (32)*].

Defining the specific entrainment rate as the entrainment rate per unit area of nozzle cross section, that is, $2\pi m_1/d_o$ in two dimensions and $2M_1/d_o^2$ for the axisymmetric case, Equation (8) indicates that the specific entrainment rate increases with u_{mf} and with L/d_o. However, since L/d_o varies as $u_o^{0.4}$ [see Equation (32)*], the ratio of the specific entrainment rate to the jet nozzle velocity (which is the ratio of the rate of fluid and particle entrainment to the rate at which fluid is supplied to the jet nozzle) decreases as u_o increases. This is shown in Table 2 for experiments 1 to 4 reported here.

Data on entrainment rates into jets in fluidized beds are difficult to obtain, and consequently there is little information in the literature. However, one datum point can be deduced from the work of Behie et al. (1971). They investigated heat transfer between a vertical jet of hot air ($d_o = 18.8$ mm, $u_o = 61$ m/s, $\rho_f = 0.91$ kg/m^3) and a well-fluidized bed of cracking catalyst ($d_p = 0.05$ mm, $\rho_p = 1\,000$ kg/m^3). By assuming that most of the jet heat was transferred to the entrained solids, they estimated that the solids loading in the jet was given by

$$\frac{\text{mass flow rate of solids in jet}}{\text{mass flow rate of gas in jet}} = 1.3$$

The mass flow rate of gas in the jet is calculated as

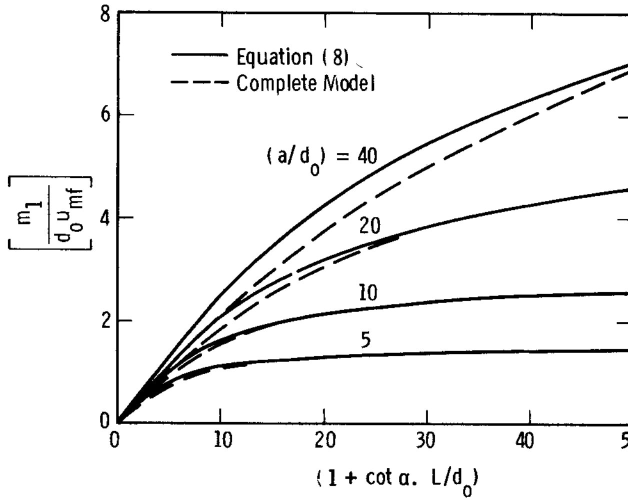

Fig. 6. Graphical representation of Equation (8) (full lines) for predicting rate of entrainment $(2\pi m_1)$ into vertical jets in fluidized beds. Broken lines show how solution of the complete model (Appendix)* differs from the prediction of Equation (8).

0.0154 kg/s, and their measurement implies that the rate of solid particle entrainment into the jet is 0.02 kg/s.

Their experiment was carried out in a bed of 610 mm diam. ($a = 610$ mm), and the end of the jet nozzle was flush with the grid plate on the center line of the bed. The jet penetration depth is calculated as $L = 668$ mm by using Equation (32)* and by taking $\alpha = 79$ deg. (Zenz and Othmer, 1960) $(1 + \cot \alpha \cdot L/d_o) = 7.9$, $(a/d_o) = 32.4$ and from Equations (5) and (9), $(M_1/\pi d_o^2\ u_{mf}) = (m_1/d_o\ u_{mf}) = 2.05$. Calculating $u_{mf} = 3.3$ mm/s for the catalyst particles using Kunii and Levenspiel's (1969) equation for small particles with $\epsilon_{mf} = 0.45$, we find that $M_1 = 7.5 \times 10^{-6}$ m^3/s, and the predicted rate of solids entrainment into the jet $= 2\pi M_1 (1 - \epsilon_{mf}) \rho_p = 0.026$ kg/s.

This predicted value of 0.026 kg/s for the rate of solids entrainment is in reasonable agreement with the value of 0.02 kg/s estimated from the data of Behie et al. (1971), indicating that Equations (8) and (9) may be used successfully for order-of-magnitude calculations.

Flow Around Grid Jets

In a conventional fluidized bed with a multiorifice distributor, the fluidizing fluid enters the bed in the form of grid jets at the orifice holes. The situation is different from those considered so far in that there is no separate supply of fluidizing fluid. It is known that particles are entrained into grid jets (Zenz, 1971), and it is postulated that there will be a corresponding entrainment of fluid into the base of these jets; the source of fluid for this entrainment must be somewhere near the end of the jet. Therefore, the suggestion is that there is circulation of particles and fluid out of the top of the grid jets and in at the base, and the two-dimensional models developed above are modified as follows.

For the particle flow field, we assume that there is a sink of strength m_1 at a height $y_1 = L/4$ above the orifice, and a source also of strength m_1 at a height $y_3 = 3L/4$ above the orifice. For the fluid flow field, there is, in addition, a source of strength m_3 at $(0, y_3)$ which is the net source of fluidizing fluid to the bed; that is

$$2\pi m_3 = a\ u_{mf} \tag{10}$$

where a is the width of the bed supplied by the orifice. As in the Appendix,* we consider infinite rows of these sources and sinks, and mirror images in the grid plate

---

* See footnote on p. 318.

Equation (32), which appears in the Appendix, is $L/d_o = 5.2\ (\rho_f d_o/\rho_p d_p)^{0.3}\ [1.3(u_o^2/g d_o)^{0.2} - 1]$, derived by Merry (1975).

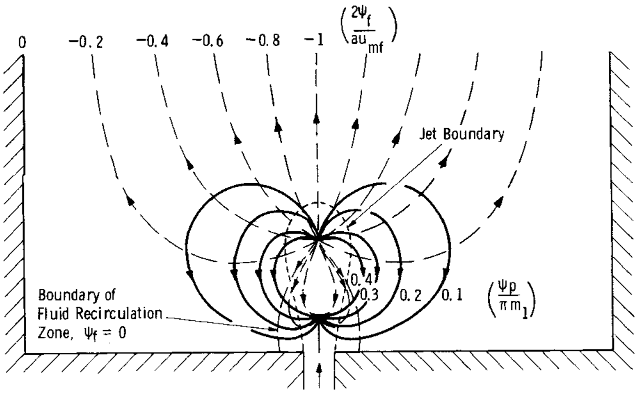

Fig. 7. Predicted streamlines for flow around a vertical grid jet corresponding to Toei's (1973) experiment. Full lines are particle streamlines [Equation (11)], and broken lines are interstitial fluid streamlines [Equation (13)].

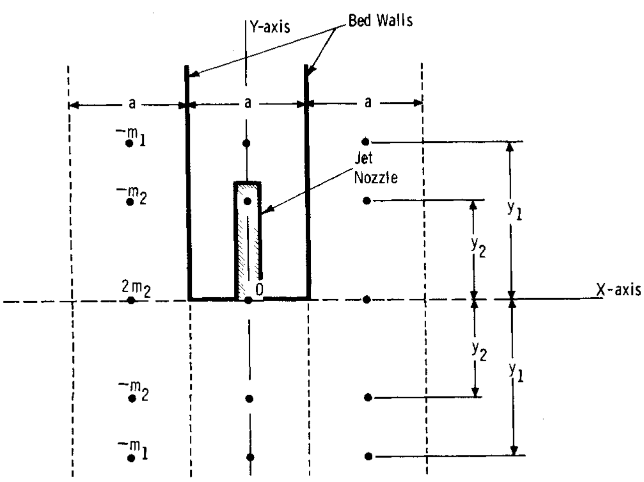

Fig. 8. Model representing solid particle flow field around a vertical jet, with sinks of strength m_1 at ($\pm na$, $\pm y_1$), sinks of strength m_2 at ($\pm na$, $\pm y_2$), and sources of strength $2m_2$ at ($\pm na$, 0) for $n = 0, 1, 2, \ldots \infty$.

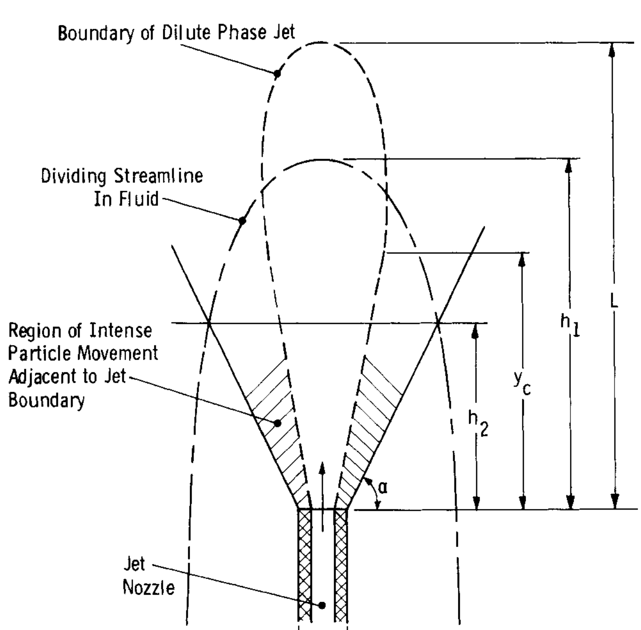

Fig. 9. Graphic representation of the interaction of particle and fluid flow fields in the vicinity of a vertical jet.

($y = 0$), so that the particle stream function is given as

$$\psi_p/m_1 = (\theta_1 - \theta_3) \quad (11)$$

and the interstitial fluid stream function as

$$\psi_f/m_1 = (\theta_1 - \theta_3) - m_3\,\theta_3/m_1 \quad (12)$$

which can be written as

$$\psi_f/m_1 = (\theta_1 - \theta_3) - a\,u_{mf}\,\theta_3/2\pi m_1 \quad (13)$$

by substituting for m_3 from Equation (10), and where θ_1 and θ_3 are defined by Equation (7) with $y_1 = L/4$ and $y_3 = 3L/4$, respectively.

If we assume that the rate of entrainment into a grid jet is the same as that into the same jet in a separately fluidized bed, we can estimate $(m_1/d_o\,u_{mf})$ from Equation (8) and so plot the particle and fluid flow fields for a given jet.

Toei (1973) studied the fluidization of a small two-dimensional bed (a = 100 mm) of glass beads (d_p = 250μm, ρ_p = 2 900 kg/m^3) with a single orifice (d_o = 5 mm) at the center of the grid plate. For an air jet (ρ_f = 1.2 kg/m^3) with a nozzle velocity u_o = 6 m/s, the jet penetration depth calculated from Equation (32)* is L = 24 mm. From α = 65 deg. (Zenz and Othmer, 1960), Equation (8) gives $(m_1/d_o\,u_{mf}) = 0.81$ so that m_1/u_{mf} = 4.05 mm. By using this value in Equations (11) and (13), the predicted particle and fluid streamlines corresponding to Toei's (1973) experiment are shown in Figure 7. van Velzen et al. (1974) deduced from their experiments in spouted beds that a considerable recirculation of gas takes place in the vicinity of the spout nozzle, and Rooney and Harrison (1974) have illustrated the similarity between grid jets and spouts, so that there is strong support for the model presented here for the particle and fluid flow fields due to a grid jet. Fluid recirculation around the jet continues around the subsequently formed bubble giving rise to the cloud around a rising bubble in a fluidized bed for which u_{mf} is less than the bubble rising velocity (Rowe, 1971). It may have little effect on heat transfer, since the heat capacity of the solids is considerably greater than that of the fluid, but it could be an important factor where chemical reaction or mass transfer occur in the jet. The ratio m_1/m_3 = 0.25 for the above calculation is the ratio of fluid recirculating to fluid percolating to the bed. Toei (1973) has recognized the importance of the grid region in fluidized bed operation and has pointed out how little is known about this part of the bed, but his model of the fluid flow field around a grid jet ignores the motion of the particles and so does not allow for the possibility of fluid recirculation.

Behie and Kehoe (1973) ignore the presence of particles in the jet in their reaction model of the grid region, arguing that the solids concentration in the jet is low. This assumption may be justified in the case of high velocity jets into fine catalyst particles, for example, in the experiments of Behie et al. (1971), in which the jet solids loading was estimated as 1.3 kg of solids/kg of gas, but it may not be valid under other conditions. In Toei's (1973) experiment, u_{mf} = 129 mm/s, and we calculate m_1 = 522 mm^2/s, particle entrainment rate into jet = 0.0026 kg/s, and fluid flow rate through jet = 0.00018 kg/s, giving a solids loading of 14.5 kg of solids/kg of gas which is an order of magnitude greater than the value obtained by Behie et al. (1971). Furthermore, Kunii (1973) and Aoyagi and Kunii (1974) have pointed out that for highly exothermic reactions, even very low concentrations of solids in dilute phase regions of the bed can have a considerable effect on overall conversion.

ACKNOWLEDGMENT

The author wishes to express his appreciation to Drs. J. L. P. Chen and D. L. Keairns for their helpful discussion, to Mr. C. Spangler who constructed the apparatus, and to Mr. J. McKenzie for his help with the photographic work.

The work was performed as part of the Westinghouse Coal Gasification Program. The project is being carried out by a six-member industry/government partnership comprising the U.S. Department of Interior's Office of Coal Research, Public Service of Indiana, Bechtel, Inc., Amax Coal Co., Peabody Coal Co./Kennecott Copper Corp., and Westinghouse Electric Corp.

NOTATION

a = bed width
A = variable defined in Equation (31)*
b = nozzle width
B = variable defined in Equation (31)*
c = length of nozzle
d_o = jet nozzle diameter
d_p = particle diameter
g = acceleration due to gravity
h_1, h_2 = heights above jet nozzle defined in Figure 9
i = square root of -1
K = permeability constant
L = jet penetration depth, Figure 9 and Equation (32)*
m = two-dimensional sink strength
m_1 = sink representing jet
m_2 = sink representing nozzle
m_3 = source representing outflow into bed, Equation (10)
M_1 = three-dimensional sink representing jet
n = integer
p_f = interstitial fluid pressure
q = flow rate
u = absolute fluid velocity
u_{mf} = absolute incipient fluidizing velocity
u_o = jet nozzle velocity
U = superficial fluid velocity
v = absolute particle velocity
w = complex potential
x = horizontal coordinate
y = vertical coordinate
y_c = height of bottom conical region of jet, Figure 9
y_n = positions of sources and sinks for $n = 0, 1, 2, 3$
z = complex variable ($= x + iy$)

Greek Letters

α = angle of internal friction
ϵ_{mf} = voidage fraction at incipient fluidization
θ = angle
θ_n = angles defined by Equation (24)* for $n = 0, 1, 2, 3$
μ = fluid viscosity
ρ_f = density of fluid
ρ_p = density of solid particles
ϕ = velocity potential
ψ = stream function
ψ_f = stream function of fluid
ψ_p = stream function of solid particles

Subscripts

c = at center line
d = at dividing streamline
o = at nozzle wall
w = at wall of bed
x = component in x direction
y = component in y direction

* See footnote on page 318.

LITERATURE CITED

Abramovich, G. N., *The Theory of Turbulent Jets*, Mass. Inst. Technol. Press, Cambridge (1963).

Aoyagi, M., and D. Kunii, "Importance of Dispersed Solids in Bubbles for Exothermic Reactions in Fluidized Beds," *Chem. Eng. Commun.*, 1, 191 (1974).

Behie, L. A., M. A. Bergougnou, and C. G. J. Baker, "Heat Transfer from a Grid Jet in a Large Gas Fluidized Bed," 21st Canadian Chemical Engineering Conf., Montreal, Oct. (1971).

Behie, L. A., and P. Kehoe, "Grid Region in a Fluidized Bed Reactor," *AIChE J.*, **19**, 1070 (1973).

Davidson, J. F., and D. Harrison, *Fluidized Particles*, Chapt. 4, Cambridge University Press, England (1963).

Halow, J. S., "Fluidized-Bed Applications," *AIChE Symposium Ser.*, **70**, No. 141, 1 (1974).

Kozin, V. E., and A. P. Baskakov, "Studies of the Jet Range in a Bed of Granular Particles," *Khim. i Tekhnol. Topliv i Masel.*, 3, 4 (1967).

Kunii, D., and O. Levenspiel, *Fluidization Engineering*, p. 73, Wiley, New York (1969).

Kunii, D., "Importance of Dispersed Solids in Bubbles for Exothermic Reactions," *AIChE Symposium Ser.*, **69**, No. 128, 24 (1973).

Lemezis, S., and D. H. Archer, "Coal Gasification for Electric Power Generation," *Combustion*, **45**, 6 (1973).

Markhevka, V. I., V. A. Basov, T. K. Melik-Akhnazarov, and D. I. Orochko, "The Flow of a Gas Jet into a Fluidized Bed," *Theor. Found. Chem. Eng.*, **5**, 80 (1971).

Merry, J. M. D., "Penetration of a Horizontal Gas Jet into a Fluidized Bed," *Trans. Inst. Chem. Engrs.*, *49*, *189* (*1971*).

———, and J. F. Davidson, "Gulf Stream Circulation in Shallow Fluidized Beds," *ibid.*, **51**, 361 (1973).

Merry, J. M. D., "Penetration of Vertical Jets into Fluidized Beds," *AIChE J.*, **21**, 507 (1975).

———, J. L.-P. Chen, and D. L. Keairns, "Design Considerations for Development of a Commercial Fluidized Bed Agglomerating Combustor/Gasifier," International Fluidization Conf., Asilomar Conf. Grounds, Calif. (June 15-20, 1975).

Milne-Thomson, L. M., *Theoretical Hydrodynamics*, 5 ed., MacMillan, New York (1968).

Rooney, N. M., and D. Harrison, "Spouted Beds of Fine Particles," *Powder Technol.*, 9, 227 (1974).

Rowe, P. N., in *Fluidization*, J. F. Davidson and D. Harrison, ed., p. 181, Academic Press, London and New York (1971).

Shakhova, N. A., "Outflow of Turbulent Jets into a Fluidized Bed," *Inzh. Fig. Zh.*, **14**, 61 (1968).

Toei, R., "Some Opinions for Modeling of Fluidized Bed," *AIChE Symposium Ser.*, **69**, No. 128, 18 (1973).

van Velzen, D., H. J. Flamm, and H. Langenkamp, "Gas Flow Patterns in Spouted Beds," *Can. J. Chem. Eng.*, **52**, 145 (1974).

Vulis, L. A., and T. A. Leont'yeva, "Co-flowing and Counter-flowing Turbulent Jets," *Izv. Akad. Nauk, Kaz.* SSSR. *Ser. Energ.*, **9**, 109 (1955).

Zenz, F. A., and D. F. Othmer, *Fluidization and Fluid-Particle Systems*, Chapt. 2, Reinhold, New York (1960).

Zenz, F. A., in *Fluidization*, J. M. Pirie, ed., p. 136, The Institution of Chemical Engineers, London, England (1968).

Zenz, F. A., in *Fluidization*, J. F. Davidson and D. Harrison, ed., p. 13, Academic Press, London and New York (1971).

Manuscript received July 31, 1975; revision received November 19 and accepted November 21, 1975.